

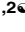
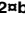
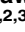


RESEARCH ARTICLE

# Arginine Thiazolidine Carboxylate Stimulates Insulin Secretion through Production of Ca<sup>2+</sup>-Mobilizing Second Messengers NAADP and cADPR in Pancreatic Islets

Dae-Ryoung Park<sup>1,2</sup> , Asif Iqbal Shawl<sup>1,2</sup> <sup>‡a</sup>, Tae-Geun Ha<sup>1,2</sup> , Kwang-Hyun Park<sup>1,2</sup> <sup>‡b</sup>, Seon-Young Kim<sup>1,2</sup>, Uh-Hyun Kim<sup>1,2,3</sup> <sup>\*</sup>

**1** Department of Biochemistry, Chonbuk National University Medical School, Jeonju, Korea, **2** National Creative Research Laboratory for Ca<sup>2+</sup> Signaling Network, Chonbuk National University, Jeonju, Korea, **3** Institute of Cardiovascular Research, Chonbuk National University, Jeonju, Korea

 These authors contributed equally to this work.

<sup>‡a</sup> Current address: Department of Emerging Materials Science, Daegu Gyeongbuk Institute of Science and Technology (DGIST), Daegu, Korea

<sup>‡b</sup> Current address: Department of Oriental Pharmaceutical Development, Nambu University, Gwangju, Korea

\* [uhkim@chonbuk.ac.kr](mailto:uhkim@chonbuk.ac.kr)



click for updates

## OPEN ACCESS

**Citation:** Park D-R, Shawl AI, Ha T-G, Park K-H, Kim S-Y, Kim U-H (2015) Arginine Thiazolidine Carboxylate Stimulates Insulin Secretion through Production of Ca<sup>2+</sup>-Mobilizing Second Messengers NAADP and cADPR in Pancreatic Islets. PLoS ONE 10(8): e0134962. doi:10.1371/journal.pone.0134962

**Editor:** Pratibha V. Nerurkar, College of Tropical Agriculture and Human Resources, University of Hawaii, UNITED STATES

**Received:** January 15, 2015

**Accepted:** July 16, 2015

**Published:** August 6, 2015

**Copyright:** © 2015 Park et al. This is an open access article distributed under the terms of the [Creative Commons Attribution License](https://creativecommons.org/licenses/by/4.0/), which permits unrestricted use, distribution, and reproduction in any medium, provided the original author and source are credited.

**Data Availability Statement:** All relevant data are within the paper and its Supporting Information files.

**Funding:** This work was supported by the National Research Foundation Grant 2012R1A3A2026453 funded by the Korean government (to U.-H.K.).

**Competing Interests:** The authors have declared that no competing interests exist.

## Abstract

Oxothiazolidine carboxylic acid is a prodrug of cysteine that acts as an anti-diabetic agent via insulin secretion and the formation of the Ca<sup>2+</sup>-mobilizing second messenger, cyclic ADP-ribose (cADPR). Here we show that a hybrid compound, arginine thiazolidine carboxylate (ATC), increases cytoplasmic Ca<sup>2+</sup> in pancreatic β-cells, and that the ATC-induced Ca<sup>2+</sup> signals result from the sequential formation of two Ca<sup>2+</sup>-mobilizing second messengers: nicotinic acid adenine dinucleotide phosphate (NAADP) and cADPR. Our data demonstrate that ATC has potent insulin-releasing properties, due to the additive action of its two components; thiazolidine carboxylate (TC) and L-arginine. TC increases glutathione (GSH) levels, resulting in cAMP production, followed by a cascade pathway of NAADP/nitric oxide (NO)/cGMP/cADPR synthesis. L-arginine serves as the substrate for NO synthase (NOS), which results in cADPR synthesis via cGMP formation. Neuronal NOS is specifically activated in pancreatic β-cells upon ATC treatment. These results suggest that ATC is an ideal candidate as an anti-diabetic, capable of modulating the physiological Ca<sup>2+</sup> signalling pathway to stimulate insulin secretion.

## Introduction

Thiazolidines are a class of heterocyclic organic compounds that has a 5-member saturated ring with a thioether group and an amine group in the 1 and 3 positions, respectively. It is a sulfur analog of oxazolidine [1]. We have previously demonstrated that a thiazolidine analog,

oxothiazolidine carboxylic acid (OTC), enhances insulin secretion in pancreatic islets [2]. The mechanism by which OTC enhances insulin secretion was explained by its ability to increase intracellular glutathione levels as a prodrug of cysteine, a rate-limiting precursor in glutathione synthesis. An increase in intracellular reducing power was able to induce CD38 dimerization and internalization, which resulted in the production of cyclic ADP-ribose (cADPR), a  $\text{Ca}^{2+}$ -mobilizing messenger [2].

L-Arginine potentiates glucose-induced insulin release [3], and arginine-derived nitric oxide (NO) has been suggested as a mediator in insulin secretion stimulated by arginine. It was shown that the potentiation of glucose-induced insulin release by arginine is a  $\text{Ca}^{2+}$ -dependent mechanism, which results from membrane depolarization and the rise of cytoplasmic  $\text{Ca}^{2+}$  in  $\beta$ -cells [4]. NO was first discovered as a mediator in vascular smooth muscle relaxation, where it induces a decrease in intracellular free calcium [ $\text{Ca}^{2+}$ ]<sub>i</sub> [5], but accumulating evidence demonstrated that treatment with NO or NO donors elicits a rise in [ $\text{Ca}^{2+}$ ]<sub>i</sub> in a variety of cells, including pancreatic  $\beta$ -cells [6–8]. Furthermore, the regulation of insulin release by arginine has been reported to be deficient in patients with type 2 diabetes mellitus [9]. These findings indicate that arginine plays a beneficial role in glucose homeostasis by targeting  $\beta$ -cells.

ADP-ribosyl cyclases (ARCs) catalyze the synthesis and hydrolysis of two  $\text{Ca}^{2+}$ -mobilizing second messengers: cADPR and nicotinic acid adenine dinucleotide phosphate (NAADP) [10–11]. ARC was first purified and cloned from the ovotestis of *Aplysia californica* [12,13]. Later, CD38, a T cell surface antigen, was found to be an ARC homolog [14], and it has been known to be a mammalian prototype of ARCs [15].

Since the first demonstration of the role of cADPR in pancreatic islets [16], its role in insulin secretion was confirmed by the demonstration of CD38-induced intracellular cADPR production [17]. Mounting evidence showed that NAADP also played a key role in the endocrine pancreas [18–20]. Our previous study demonstrated that glucagon-like peptide-1 (GLP-1)-mediated  $\text{Ca}^{2+}$  signals in insulin secretion from pancreatic  $\beta$ -cells is a cooperative process between the actions of cADPR and NAADP [21]. The initial phase of the GLP-1-activated  $\text{Ca}^{2+}$  signals is due to NAADP-mediated  $\text{Ca}^{2+}$  mobilization from acidic stores, while the second, maintained phase is attributable to the cADPR-mediated  $\text{Ca}^{2+}$  signal mediated through the endoplasmic reticulum. In support of these data,  $\beta$ -cells isolated from CD38<sup>-/-</sup> mice showed reduced production of NAADP and cADPR after activation by GLP-1, indicating a partial dependence on CD38.

In the present study, we synthesized arginine thiazolidine carboxylate (ATC), a hybrid compound derived from a prodrug of cysteine, and examined its effects on insulin secretion and  $\text{Ca}^{2+}$  signaling in pancreatic islets. We found that the hybrid molecule displayed higher potency in inducing insulin secretion as well as NAADP and cADPR production when compared to its analogs or precursor components.

## Materials and Methods

### Reagents

Dulbecco's Modified Eagle's medium (DMEM) containing low glucose, and antibiotics were from GIBCO (Grand Island, NY, USA). (Rp)-8-pCPT-cGMP-S was purchased from Calbiochem (Darmstadt, Germany). All other reagents were obtained from Sigma (Sigma Aldrich, St Louis, USA). Recombinant nicotinic acid mononucleotide adenylyltransferase (NMN-AT) was a gift from Dr. S. W. Suh [22].

## Synthesis of arginine thiazolidine carboxylate

Thiazolidine-2-carboxylic acid or thiazolidine-4-carboxylic acid (0.94 mmol) was dissolved in methanol (25 mL) under stirring. The solution was stirred at room temperature for 10 min. During stirring *L*-arginine hydrochloride (0.94 mmol) in distilled water (5 mL) was added dropwise into flask. The reaction mixture was stirred at 50 °C until obtain clear solution. Methanol was removed by rotary evaporator. The obtained solid was dried under vacuum. The solid was suspended in acetone (100 mL) and stirred vigorously. The solid was filtered and dried under vacuum, to give arginine thiazolidine-2-carboxylate or arginine thiazolidine-4-carboxylate as a white solid. <sup>1</sup>H- and <sup>13</sup>C-NMR spectra were recorded on Jeol 400 MHz spectrometer. Chemical shifts are shown in  $\delta$  values (ppm). Arginine thiazolidine-2-carboxylate; Yield: 78.1%; <sup>1</sup>H NMR (400 MHz, D<sub>2</sub>O)  $\delta$  5.03 (s, 1H), 3.67–3.61 (m, 2H), 3.56–3.50 (m, 1H), 3.13–3.08 (m, 4H), 1.79–1.72 (m, 2H), 1.63–1.44 (m, 2H); <sup>13</sup>C NMR (100 MHz, D<sub>2</sub>O)  $\delta$  175.2, 172.7, 157.7, 63.4, 55.3, 50.4, 41.6, 30.6, 28.5, 24.9; ESI MS: *m/z* 308.1 (M + H)<sup>+</sup>. Arginine thiazolidine-4-carboxylate; Yield: 67.9%; <sup>1</sup>H NMR (400 MHz, D<sub>2</sub>O)  $\delta$  4.22 (d, *J* = 9.76, 1H), 3.86 (d, *J* = 9.76, 1H), 3.62 (t, *J* = 5.84, 1H), 3.50 (t, *J* = 7.8, 1H), 3.16–3.09 (m, 3H), 2.69–2.64 (m, 1H), 1.79–1.74 (m, 2H), 1.63–1.54 (m, 2H); <sup>13</sup>C NMR (100 MHz, D<sub>2</sub>O)  $\delta$  178.7, 175.5, 157.6, 68.2, 55.2, 53.4, 41.4, 37.2, 28.5, 24.7; ESI MS: *m/z* 308.1 (M + H)<sup>+</sup>.

## Animals

Mice with genetic background ICR were inbred in the Animal Facility of Chonbuk National University Medical School. CD38 knockout mice (*Cd38*<sup>-/-</sup>; B6.129P2-*Cd38*<sup>tm/Lud</sup>) were purchased from Jackson Laboratory (Bar Harbor, ME). Male C57BL/KsJ-db/db mice (7 weeks old) were purchased from Clea Japan (Tokyo, Japan). All animal-based investigations were designed and performed in accordance with the Guide for the Care and Use of Laboratory Animals published by the National Institutes of Health (NIH Pub. No. 85–23, revised 1996) [23]. The entire project was reviewed and approved by the Institutional Animal Care and Use Committee of the Chonbuk National University Medical School (CBU 2013–0009).

## Preparation of islets

Pancreatic islets were isolated from ICR background mice, weighing 25–30 g, using a collagenase method, except Krebs-Ringer bicarbonate buffer (KRB buffer in mmol/L: 2 CaCl<sub>2</sub>, 2.8 glucose, 145 NaCl, 1.19 KCl, 2.54 MgCl<sub>2</sub>, 1.19 KH<sub>2</sub>PO<sub>4</sub>, 5 NaHCO<sub>3</sub>, 20 HEPES, pH 7.3), was used instead of Krebs-Ringer buffer. Briefly, sacrifice animal by cervical dislocation. Make a V-incision starting at the genital area of the mouse. Pancreas was distended by infusion of KRB buffer containing 0.15 mg/ml type V collagenase through the bile duct. Incubate for 20–25 minutes at 37°C in water-bath. Islets were isolated, washed with KRB buffer, resuspend the pellet in ficoll and centrifuge, islets were handpicked to eliminate any remaining exocrine tissue and stabilized by culturing overnight at 37°C in a humidified incubator (95% air, 5% CO<sub>2</sub>) in low glucose (5 mmol/L) DMEM supplemented with 10% (v/v) fetal bovine serum (FBS), 100 units/ml penicillin G, and 100  $\mu$ g/mL streptomycin (culture media).

## Measurement of [Ca<sup>2+</sup>]<sub>i</sub>

Dispersed  $\beta$ -cells obtained by trituration of islets with a pipette were seeded on confocal dishes and cultured in culture media.  $\beta$ -cells were identified on the basis of their large diameter and granular appearance. Adhered cells were washed with KRB buffer containing 0.1% BSA and loaded with 1  $\mu$ M Fluo-3 AM (Molecular Probe, Eugene, OR) at 37°C for 30 min. After washing with KRB buffer containing 0.1% BSA, an appropriate amount of glucose was

supplemented. Changes in  $[Ca^{2+}]_i$  were determined at 488/530 nm excitation/emission by air-cooled argon laser system [24]. The emitted fluorescence at 530 nm was collected using a photomultiplier. One image every 3 sec was scanned using confocal microscope (Nikon, Japan).  $[Ca^{2+}]_i$  calculation was performed by using an equation given by Tsein *et al* [25], i.e.  $[Ca^{2+}]_i = K_d(F - F_{min}) / (F_{max} - F)$ , where  $K_d$  is 450 nM for Fluo-3 and  $F$  is the observed fluorescence levels. Each tracing was calibrated for the maximal intensity ( $F_{max}$ ) by addition of 8  $\mu$ mol/L ionomycin and for the minimal intensity ( $F_{min}$ ) by addition of 50 mmol/L EGTA at the end of each measurement. Fluorescence in  $\beta$ -cells was determined as described previously [21].

### Measurement of cAMP production

Levels of cAMP were determined in whole islets as described previously [26]. Batches of 40 islets were incubated for 15 min at 37°C in KR buffer supplemented with 0.1% BSA, 400  $\mu$ mol/L ATC, 12 mmol/L glucose. cAMP content of acetylated samples was measured using a commercially available cAMP ELISA assay kit (Enzo Life Sciences, Farmingdale, NY, USA).

### Measurement of intracellular cADPR concentration

Cyclic enzymatic assay was performed to measure cADPR levels as described previously [27]. Briefly 40–50 islets were treated with 0.6 mol/L perchloric acid (PCA) under sonication. Precipitates were removed by centrifugation at 20,000  $\times g$  for 10 min at 4°C. To remove PCA, aqueous sample was mixed with a solution containing 1,1,2-trichlorotrifluoroethane and tri-*n*-octylamine in the ratio of 3:1. After centrifugation for 10 min at 1500  $\times g$ , the aqueous layer was collected and neutralized with 20 mmol/L sodium phosphate buffer (pH 8.0). To remove contaminating nucleotides, the samples were incubated overnight with 2.5 mmol/L  $MgCl_2$  and following enzymes in 20 mmol/L sodium phosphate buffer (pH 8.0) at 37°C: 0.44 unit/mL nucleotide pyrophosphatase, 12.5 unit/mL alkaline phosphatase and 0.625 unit/mL NADase. Enzymes were removed by filtration using Centricon-3 filters. To convert cADPR to  $NAD^+$ , the samples (0.1 mL/tube) were incubated with 50  $\mu$ l of a cycling reagent containing 0.3  $\mu$ g/mL *Aplysia* ADPR cyclase, 30 mmol/L nicotinamide, and 100 mmol/L sodium phosphate (pH 8.0), at room temperature for 15 min. The samples were further incubated with the cycling reagent (0.1 mL) containing 2% ethanol, 100  $\mu$ g/mL alcohol dehydrogenase, 20  $\mu$ mol/L resazurin, 10  $\mu$ g/mL diaphorase, 10  $\mu$ mol/L riboflavin 5-phosphate, 10 mmol/L nicotinamide, 0.1 mg/mL BSA and 100 mmol/L sodium phosphate (pH 8.0) for 2–4 hours at room temperature. An increase in resorufin fluorescence was measured at 544 nm excitation and 590 nm emission using a fluorescence microplate reader (Molecular Devices Corp., Spectra-Max GEMINI). Level of cADPR was measured using a cyclic enzymatic assay as described previously. For the experiment, *Neurospora crassa* NADase and *Aplysia* ARC were purified according to the methods described by Cho *et al* [28] and Lee *et al* [29], respectively.

### Measurement of intracellular NAADP concentration

Cyclic enzymatic assay was performed to measure NAADP levels as described previously [27]. Briefly 40–50 islets were treated with 0.6 mol/L PCA under sonication. Precipitates were removed by centrifugation at 20,000  $\times g$  for 10 min at 4°C. To remove PCA, aqueous sample was mixed with a solution containing 1,1,2-trichlorotrifluoroethane and tri-*n*-octylamine in the ratio of 3:1. After centrifugation for 10 min at 1500  $\times g$ , the aqueous layer was collected and neutralized with 20 mmol/L sodium phosphate buffer (pH 8.0). To remove contaminating nucleotides, the samples were incubated overnight with 2 mmol/L  $MgCl_2$ , 1 mmol/L sodium fluoride and 0.1 mmol/L inorganic pyrophosphate and following enzymes in 20 mmol/L

sodium phosphate buffer (pH 8.0) at 37°C: 2.5 unit/mL Apyrase, 0.16 mg/mL NMN-AT and 0.125 unit/mL NADase. Enzymes were removed by filtration using Centricon-3 filters. Unlike conversion of cADPR to NAD<sup>+</sup>, NAADP is first converted to nicotinic acid adenine dinucleotide (NAAD) by addition of 10 unit/ml of alkaline phosphatase overnight at 37°C. Enzymes were removed by filtration using Centricon-3 filters. NAAD is further converted to NAD by the 0.2 mg/mL NMN-AT. NMN-AT is a reversible enzyme and can use NAAD as well as NAD as substrate. NMN-AT converts NAAD to nicotinic acid mononucleotide (NAMN) and ATP in the presence of 0.5 mmol/L inorganic pyrophosphate (PPi). 0.2 mmol/L NMN is included which combines with ATP to form NAD in presence of 2 mmol/L MgCl<sub>2</sub>, 10 mmol/L nicotinamide, 2 mmol/L sodium fluoride and 100 mmol/L Tris-HCl (pH-8.0) at room temperature for 30 min. The samples were further incubated with the cycling reagent containing 2% ethanol, 100 µg/ml alcohol dehydrogenase, 20 µmol/L resazurin, 10 µg/mL diaphorase, 10 µmol/L riboflavin 5-phosphate, 10 mmol/L nicotinamide, 0.1 mg/mL BSA and 100 mmol/L sodium phosphate (pH 8.0) for 2–4 h at room temperature. An increase in resorufin fluorescence was measured at 544 nm excitation and 590 nm emission using a fluorescence microplate reader (Molecular Devices Corp., Spectra-Max GEMINI). Level of cADPR was measured using a cyclic enzymatic assay as described previously. For the experiment, *Neurospora crassa* NADase and *Aplysia* ARC were purified according to the methods described by Cho *et al* [28] and Lee *et al* [29], respectively.

### cGMP enzyme-linked immunoassay

Cultured isolated islets (25 islets/sample) were washed twice with fresh medium. Ice-cold HCl (final concentration 0.1 M) was added to stop the reaction. Samples were frozen and thawed three times, sonicated, and centrifuged at 500 rpm for 10 min. Supernatants were assayed for cGMP by enzyme-linked immunoassay kit (Cell Signaling Technology, Inc., Massachusetts, USA) [30].

### Nitrite measurement

Biologically produced NO is rapidly oxidized to nitrite and nitrate in aqueous solutions [31,32]. Nitrite concentrations in the cell-free culture supernatants, therefore, served as a reflection of NO production and were measured using a previously described colorimetric assay [33]. Following overnight incubation at 37°C in a humidified 95% air/5% CO<sub>2</sub> atmosphere, nitrite concentration was measured from 30 islets in KR buffer with/without ATC. Briefly, 50-µl aliquots of supernatants dispensed into 96-well microtiter plates (flat bottom) (SPL, Life Sciences, Pocheon, Republic of Korea) were incubated with 100 µl of a 1:1 mixture of 1% sulfanilamide (Sigma Aldrich, St Louis, USA) in 30% acetic acid and 0.1% *N*-(1-naphthyl)ethylene-diamine dihydrochloride (Sigma Aldrich, St Louis, USA) in 60% acetic acid at room temperature. After 5 min, absorbance was measured at 570 nm using a micro plate reader (BioRad XMark, Microplate Spectrophotometer, Japan). Concentrations were determined from a linear standard curve obtained from serial concentrations (6.25–200 mM) of sodium nitrite (Sigma Aldrich, St Louis, USA) in working medium. Results of triplicate measurements were presented as means ± SD.

### Glucose Tolerance Test

Male C57BL/KsJ-db/db mice (7 weeks old) were purchased from Clea Japan (Tokyo, Japan). Mice were maintained in an environmentally controlled room with a 12-h light-dark cycle and were allowed free access to diet and a specific pathogen-free water. For glucose tolerance test, mice were fasted overnight and received single oral administration of various concentrations of ATC (0–40 mg/kg). Five h later, mice were injected with glucose (0.5 g/kg, intraperitoneally),



and blood samples were taken at various time points (0–120 min). Blood glucose levels were measured by the glucose oxidase method using a glucose analyzer (Lifescan, Inc., Milpitas, CA), and serum insulin levels were determined using a radioimmunoassay kit (Amersham Biosciences, Inc.).

## Statistical analysis

Data represent means  $\pm$  standard error of the mean (SEM) of at least three separate experiments. Statistical analysis was performed using Student's *t*-test or Repeated measures ANOVA. A value of  $p < 0.05$  was considered significant.

## Results

### Design and synthesis of an anti-diabetic prodrug

The effects of arginine and thiazolidine carboxylic acid (TC) in promoting insulin secretion in pancreatic islets prompted us to develop an anti-diabetic hybrid prodrug (See the chemical structures; [S1 Fig](#)). L-arginine, a substrate for nitric oxide (NO) synthase, has been known to increase insulin secretion [3], and an analog of TC, oxothiazolidine-4-carboxylic acid (OTC), has also been known to enhance insulin secretion [2]. Before synthesizing a hybrid compound from the two precursor molecules, we compared the potency of two different TCs, thiazolidine-2-carboxylic acid (T2C) [34] and thiazolidine-4-carboxylic acid (T4C) [35], in their ability to generate intracellular glutathione (GSH) in islets, since intracellular GSH generation by TCs enhances insulin secretion [2]. GSH generation induced by T2C was higher than that by T4C ([S2 Fig](#)). Thus, we chose T2C for the synthesis of an arginine salt of thiazolidine-2-carboxylic acid (ATC), and used this ATC as a hybrid prodrug throughout the study.

### ATC displayed greater potency in inducing $\text{Ca}^{2+}$ signaling and insulin secretion when compared to precursor and analog molecules

To obtain a dose-response curve of ATC, we performed experiments of cADPR and NAADP production with various dose of ATC (100, 400, 700  $\mu\text{M}$  and 1 mM). Since our data showed that 400  $\mu\text{M}$  ATC resulted in a plateau of cADPR and NAADP production ([S3 Fig](#)), we used 400  $\mu\text{M}$  ATC in all experiments through the present work. In order to compare the potency of precursors and hybrid compounds,  $[\text{Ca}^{2+}]_i$  was measured in islets following treatment with the following agents: ATC (400  $\mu\text{M}$ ), OTC (1 mM), T2C (400  $\mu\text{M}$ ), arginine (400  $\mu\text{M}$ ), and arginine plus T2C. T2C and arginine induced a  $\text{Ca}^{2+}$  rise with less potency when compared to ATC ([Fig 1A](#)). Treatment of pancreatic  $\beta$ -cells with 400  $\mu\text{M}$  ATC induced a long lasting  $\text{Ca}^{2+}$  increase, which was also higher in amplitude, even when compared to higher concentration of OTC (1 mM) ([Fig 1B](#)).

Based on our previous findings that OTC induces CD38-mediated  $\text{Ca}^{2+}$  signalling, resulting in insulin secretion [2], we examined whether the agents induced NAADP and cADPR production. ATC strongly induced the production of both NAADP and cADPR, compared to OTC, T2C, arginine, or arginine plus T2C ([Fig 1C and 1D](#)), indicating that ATC is a potent inducer of NAADP and cADPR formation, resulting in a rise in  $\text{Ca}^{2+}$ . Arginine produced only cADPR and no NAADP, while other agents induced the production of both messengers to degrees comparable to their  $\text{Ca}^{2+}$  signalling potency. ATC-induced insulin secretion was significantly higher than those induced by OTC, T2C, or arginine, and it was comparable to that of arginine plus T2C ([Fig 1E](#)). Finally, to examine the effects of ATC on glucose levels *in vivo*, we treated mice with 5, 10, and 20 mg/kg ATC. Plasma glucose levels in mice subjected to a glucose

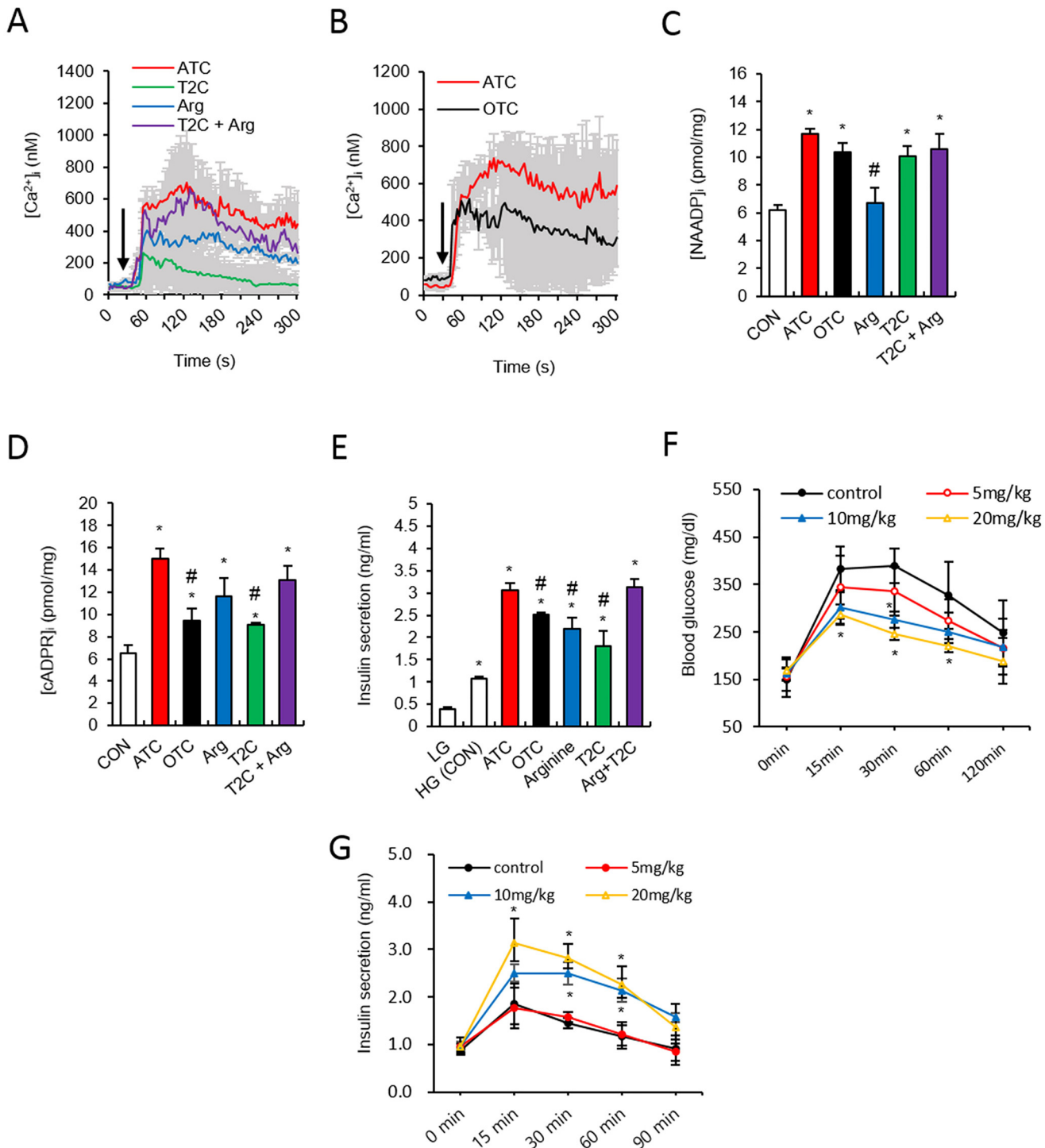


**Fig 1. ATC induces insulin secretion via cADPR/NAADP-dependent  $Ca^{2+}$  signals in pancreatic  $\beta$  cell.** (A) Representative tracing of the  $Ca^{2+}$  response to ATC (400  $\mu$ M), Arginine (400  $\mu$ M) (AG), Thiazolidine-2-carboxylic acid (400  $\mu$ M) (T2C) and T2C + Arg treatments. (B) Representative tracing of the  $Ca^{2+}$  response to ATC (400  $\mu$ M) and OTC (1 mM) treatments. (C) Comparisons of NAADP formation among ATC, OTC, Arg, T2C and T2C + AG treatment. (D) Comparisons of cADPR formation among ATC, OTC, Arg, T2C and T2C + Arg treatment. (E) Comparisons of insulin secretion among ATC, OTC, Arg, T2C and T2C + AG treatment. (F) Blood glucose levels in vehicle (closed circle,  $n = 5$ )- and ATC (5 mg/kg; open circle,  $n = 5$ , 10 mg/kg; closed triangle,  $n = 5$ , 20 mg/kg; open triangle,  $n = 5$ )-treated *db/db* mice following intraperitoneal injection of glucose after overnight fasting. (G) Plasma insulin levels during intraperitoneal glucose tolerance testing in vehicle (closed circle,  $n = 5$ )- and ATC (5 mg/kg; open circle,  $n = 5$ , 10 mg/kg; closed triangle,  $n = 5$ , 20 mg/kg; open triangle,  $n = 5$ )-treated *db/db* mice. \*,  $P < 0.05$  versus CON level. #,  $P < 0.05$  versus ATC treated level. All data are expressed as the Mean  $\pm$  SEM.

doi:10.1371/journal.pone.0134962.g001

challenge after an overnight fast were significantly ameliorated by treatment with 10 mg/kg ATC or above, and plasma insulin levels were significantly increased (Fig 1F and 1G).

### ATC induces $\text{Ca}^{2+}$ rise via NAADP and cADPR formation

Because ATC was found to induce both NAADP and cADPR production, we examined the time course for the production of both  $\text{Ca}^{2+}$  second messengers. NAADP formation, reaching its plateau at 15 sec, preceded cADPR formation, with its peak at 30 sec (Fig 2A). The ATC-mediated signalling pathway was examined by determining changes in ATC-induced  $[\text{Ca}^{2+}]_i$ , and NAADP and cADPR levels under various conditions. The ATC-induced  $\text{Ca}^{2+}$  rise was abolished by pretreatment of cells with Ned19 (100  $\mu\text{M}$ ), a NAADP receptor antagonist, but not with XeC (2  $\mu\text{M}$ ), an  $\text{IP}_3$  receptor blocker. Pretreatment of cells with a cADPR antagonist, 8-Br-cADPR, only affected the sustained  $\text{Ca}^{2+}$  rise, while the initial rise remained intact (Fig 2B). Similarly, pretreatment with high concentration of ryanodine (20  $\mu\text{M}$ ) as a ryanodine receptor blocker resulted in an inhibition of the later phase of ATC-induced  $\text{Ca}^{2+}$  signals (S4 Fig). We supposed the existence of a store-operated  $\text{Ca}^{2+}$  entry (SOCE) mechanism in ATC-induced sustained  $\text{Ca}^{2+}$  signalling. To test this notion, we treated pancreatic islets with ATC in  $\text{Ca}^{2+}$  free condition and found only a  $\text{Ca}^{2+}$  transient, presumably due to  $\text{Ca}^{2+}$  mobilization via the actions of NAADP and cADPR. The addition of extracellular  $\text{Ca}^{2+}$  resulted in sustained  $\text{Ca}^{2+}$  signals, indicating that the depletion of  $\text{Ca}^{2+}$  stores induced  $\text{Ca}^{2+}$  entry (Fig 2C). SOCE involvement in ATC-induced sustained  $\text{Ca}^{2+}$  signalling was confirmed by evidence that the ATC-mediated sustained  $\text{Ca}^{2+}$  rise was blocked by pretreatment of cells with SKF96365 (100  $\mu\text{M}$ ), a SOCE blocker (Fig 2D). NAADP formation was not affected by preincubation with 8-Br cADPR, an antagonistic analogue of cADPR, confirming that cADPR follows NAADP formation.  $\text{Ca}^{2+}$  free conditions, XeC,  $\text{IP}_3$  receptor antagonists, and SKF96365 did not block ATC-induced NAADP formation (Fig 2E). On the other hand, ATC-induced cADPR formation was blocked by the NAADP receptor antagonist, Ned19. However, XeC,  $\text{IP}_3$  receptor antagonists, SKF96365, SOCE blockers, and  $\text{Ca}^{2+}$  free conditions did not affect cADPR formation (Fig 2F). ATC-induced insulin secretion was blocked by Ned19, 8-Br-cADPR, extracellular  $\text{Ca}^{2+}$  free condition, and SKF96365, though XeC did not affect ATC-induced insulin release (Fig 2G). Together, these results suggest that ATC induces the sequential production of NAADP and cADPR, followed by SOCE for sustained  $\text{Ca}^{2+}$  signalling, ultimately resulting in insulin secretion.

### ATC-induced NAADP and cADPR formation is dependent on cAMP

Treatment with TC analogs increases intracellular GSH, which in turn induces an increase in cAMP levels [35,36]. We examined the effects of ATC treatment on cAMP production and found that ATC induced cAMP production (Fig 3A). The ATC-induced cAMP production was not affected by  $\text{Ca}^{2+}$  signaling inhibitors, XesC, NED19, or 8-Br-cADPR, suggesting that cAMP generation is located upstream to ATC-induced  $\text{Ca}^{2+}$  signaling (Fig 3B). Pretreatment with H89 (10  $\mu\text{M}$ ), a PKA inhibitor, blocked the ATC-induced  $\text{Ca}^{2+}$  rise, confirming that cAMP has a role in ATC-induced  $\text{Ca}^{2+}$  signaling (Fig 3A). To test the possibility that cAMP is a mediator in the ATC-induced production of  $\text{Ca}^{2+}$  signaling messengers, we measured ATC-induced production of NAADP and cADPR in the absence or presence of a PKA inhibitor or cAMP antagonist. Pretreatment of islets with H89 or Rp-cAMP (100  $\mu\text{M}$ ) blocked both the NAADP and cADPR formation that was induced by ATC (Fig 3C and 3D). ATC-induced glutathione synthesis was not affected by cAMP antagonists or  $\text{Ca}^{2+}$  signaling inhibitors, XesC, NED19, or 8-Br-cADPR (Fig 3E), while cAMP formation was blocked by the glutathione-depleting compound, diethyl maleate (DEM, 50  $\mu\text{M}$ ) (Fig 3F). These findings suggest that



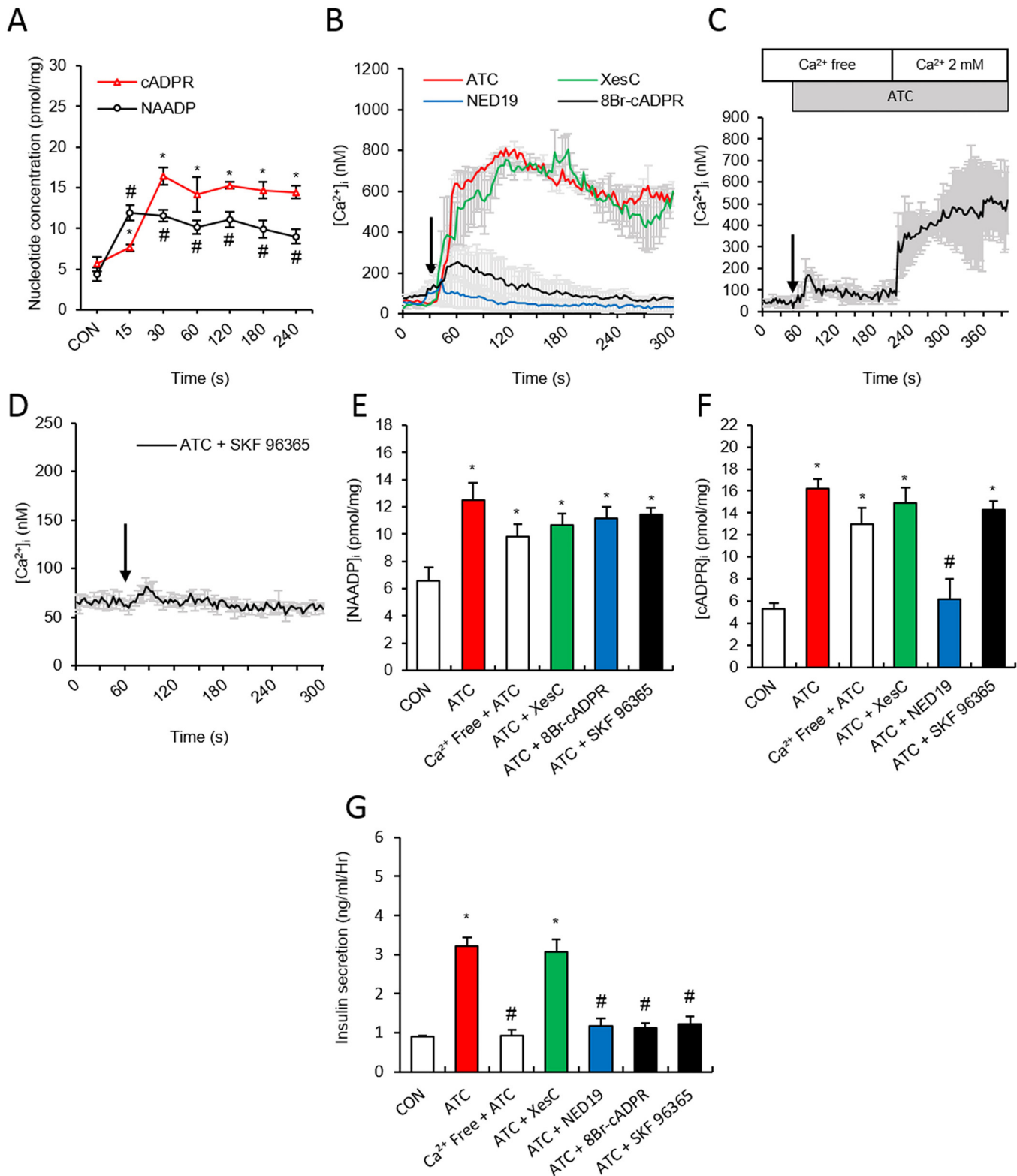


**Fig 2. ATC-induced NAADP and cADPR formation and involvement of SOCE in ATC-induced Ca<sup>2+</sup> signaling in pancreatic  $\beta$  cell.** (A) Time course of NAADP and cADPR production following ATC treatment (B) Effect of Ca<sup>2+</sup> second messenger inhibitors on ATC-induced Ca<sup>2+</sup> signals. XesC (2  $\mu$ M), Ned19 (100  $\mu$ M) and 8-Br-cADPR (100  $\mu$ M) were used. (C) Representative tracings of the Ca<sup>2+</sup> response to ATC in the absence and presence of extracellular Ca<sup>2+</sup>. (D) Representative tracings of the Ca<sup>2+</sup> response to ATC in the presence of SKF 96365 (10  $\mu$ M) (E and F) Effect of Ca<sup>2+</sup> second messenger inhibitors on

ATC-induced cADPR and NAADP formation. **(G)** Effect of  $\text{Ca}^{2+}$  second messenger inhibitors on ATC-induced insulin secretion. \*,  $P < 0.05$  versus CON level. #,  $P < 0.05$  versus ATC treated level. All data are expressed as the Mean  $\pm$  SEM.

doi:10.1371/journal.pone.0134962.g002

glutathione induces cAMP formation. Glutathione-depletion by DEM blocked NAADP and cADPR formation (Fig 3G and 3H). Consequently, DEM, as well as H89 and Rp-cAMP, inhibited ATC-induced insulin secretion (Fig 3I).

## ATC induced insulin secretion via the NO-cGMP pathway

Since arginine stimulates insulin release from pancreatic islets [3], we examined the effects of ATC as an arginine donor in inducing insulin secretion. Pretreatment of cells with L-NAME (5 mM), an inhibitor of NOS, blocked the ATC induced  $\text{Ca}^{2+}$  rise (Fig 4A). When we measured nitrite as an indicator of NO production, ATC induced a significant rise in nitrite levels when compared to high glucose alone. ATC-induced nitrite levels were comparable to those induced by arginine (Fig 4B). ATC-induced nitrite levels were not affected by pretreatment with XeC or 8-Br-cADPR, while L-NAME and Ned19 blocked nitrite formation, suggesting that NO formation is dependent on NAADP formation (Fig 4B). L-NAME only blocked ATC-induced cADPR formation, leaving the NAADP formation intact (Fig 4D and 4E), indicating that NO production is downstream to NAADP formation, and that NO plays a role in cADPR formation.

NO has been known to activate guanylyl cyclase to produce cGMP [37], which is a second messenger in the production of cADPR [38]. Therefore, it is assumed that the NO-cGMP pathway lies upstream to cADPR formation. To test this assumption, we examined the effects of a cGMP antagonistic analog, Rp-8-pCPT-cGMPS (20  $\mu\text{M}$ ), on NAADP and cADPR formation, and found that it blocked only cADPR formation (Fig 4D and 4E). These findings suggest that cGMP plays a role in cADPR formation in ATC-induced  $\text{Ca}^{2+}$  signaling. L-NAME, as well as Rp-8-pCPT-cGMPS, blocked ATC-induced insulin secretion (Fig 4 F). These data show that the NO-cGMP pathway plays an essential role in the ATC-induced insulin secretion.

## Role of nNOS in ATC-mediated $\text{Ca}^{2+}$ signalling

Since our data showed that L-NAME inhibited ATC-induced  $\text{Ca}^{2+}$  signalling (Fig 4A), we investigated which isoform(s) of NOS were involved. ARL17477 (30  $\mu\text{M}$ ), a nNOS inhibitor, blocked the ATC-induced  $\text{Ca}^{2+}$  rise, while 1400W (100  $\mu\text{M}$ ), an iNOS inhibitor, did not block the ATC-induced  $\text{Ca}^{2+}$  rise (Fig 5A). The effect of NOS inhibitors on ATC-induced NO formation correlated with our data on  $\text{Ca}^{2+}$  (Fig 5B). NAADP formation was not affected by NOS inhibitors (Fig 5C), while cADPR formation was completely inhibited by ARL 17477 (Fig 5D). Knockdown of nNOS using lentiviral particles confirmed the pharmacological data, as evidenced by showing that ATC-induced NO formation and  $\text{Ca}^{2+}$  rise was completely inhibited by nNOS knockdown (Fig 5E and 5F). ATC-induced NAADP formation was not blocked by nNOS knockdown (Fig 5G), whereas cADPR formation was inhibited by knockdown of nNOS (Fig 5H). Finally, the effects of knockdown and pharmacological inhibition of NOS isoforms on ATC-induced insulin release mirrored similar inhibitory patterns seen in  $\text{Ca}^{2+}$  signalling, cADPR formation, and NO formation (Fig 5I).

## ATC-induced insulin secretion is dependent on $\text{Ca}^{2+}$ signalling that is mediated by cADPR, which is produced by CD38

Since we have shown that OTC enhances CD38 internalization and results in cADPR production [2], we examined whether ATC-mediated  $\text{Ca}^{2+}$  signals are dependent on CD38 by

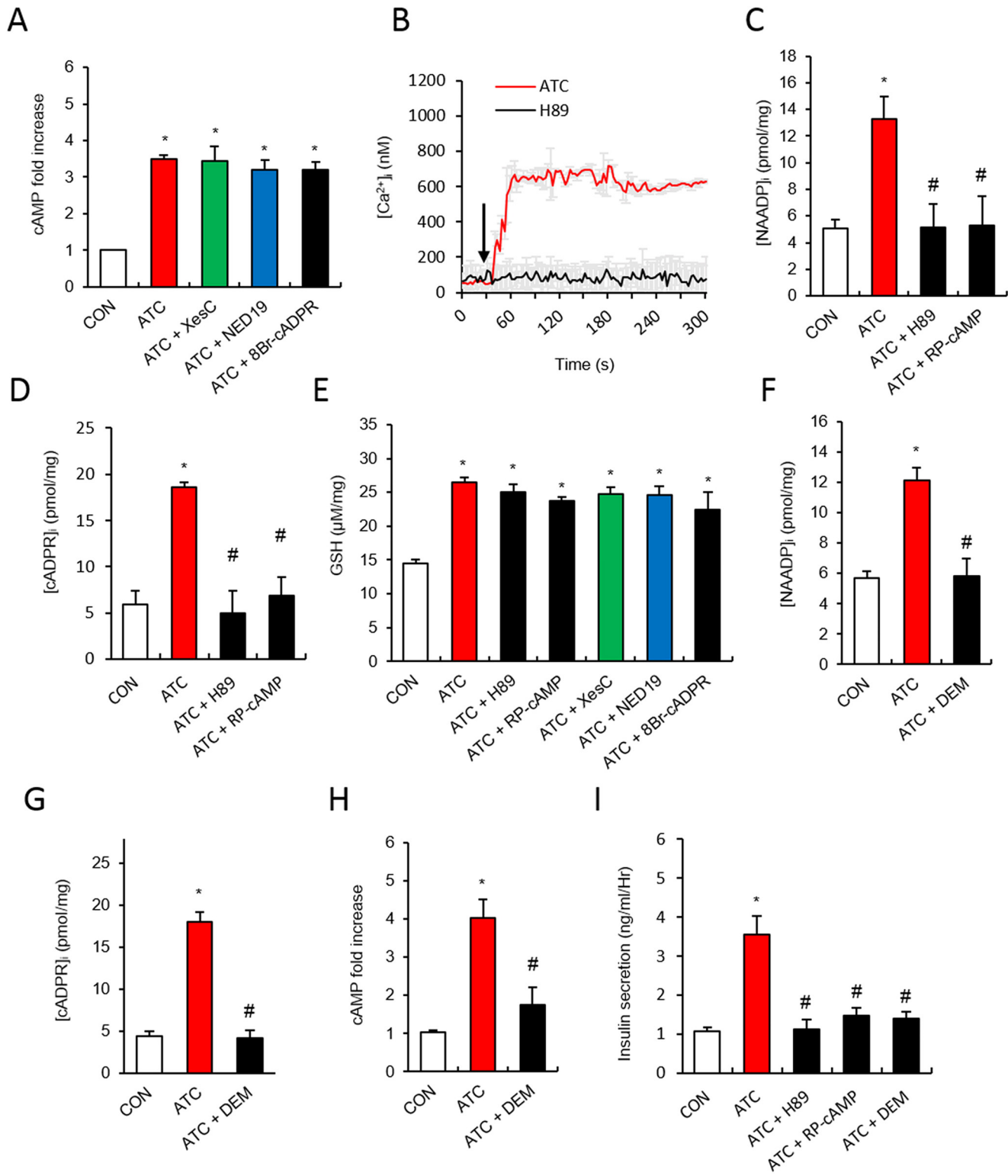


**Fig 3. ATC-induced NAADP and cADPR formation in a cAMP-dependent manner in pancreatic  $\beta$  cell.** (A) Effect of H89 (10  $\mu$ M) on ATC-induced  $Ca^{2+}$  signals. (B) Effect of  $Ca^{2+}$  second messenger inhibitors on ATC-induced cAMP formation. (C and D) Effect of H89 and Rp-cAMP (100  $\mu$ M) on ATC-induced cADPR and NAADP formation. (E) Effect of  $Ca^{2+}$  second messenger inhibitors and cAMP antagonist on ATC-induced GSH formation. (F-H) Effect of GSH inhibitor, Diethyl Maleate (DEM) (50  $\mu$ M) on ATC-induced formation of cAMP, cADPR and NAADP. (I) Inhibitory effect of cAMP antagonists or DEM on ATC-induced insulin secretion. \*,  $P < 0.05$  versus CON level. #,  $P < 0.05$  versus ATC treated level. All data are expressed as the Mean  $\pm$  SEM.

doi:10.1371/journal.pone.0134962.g003

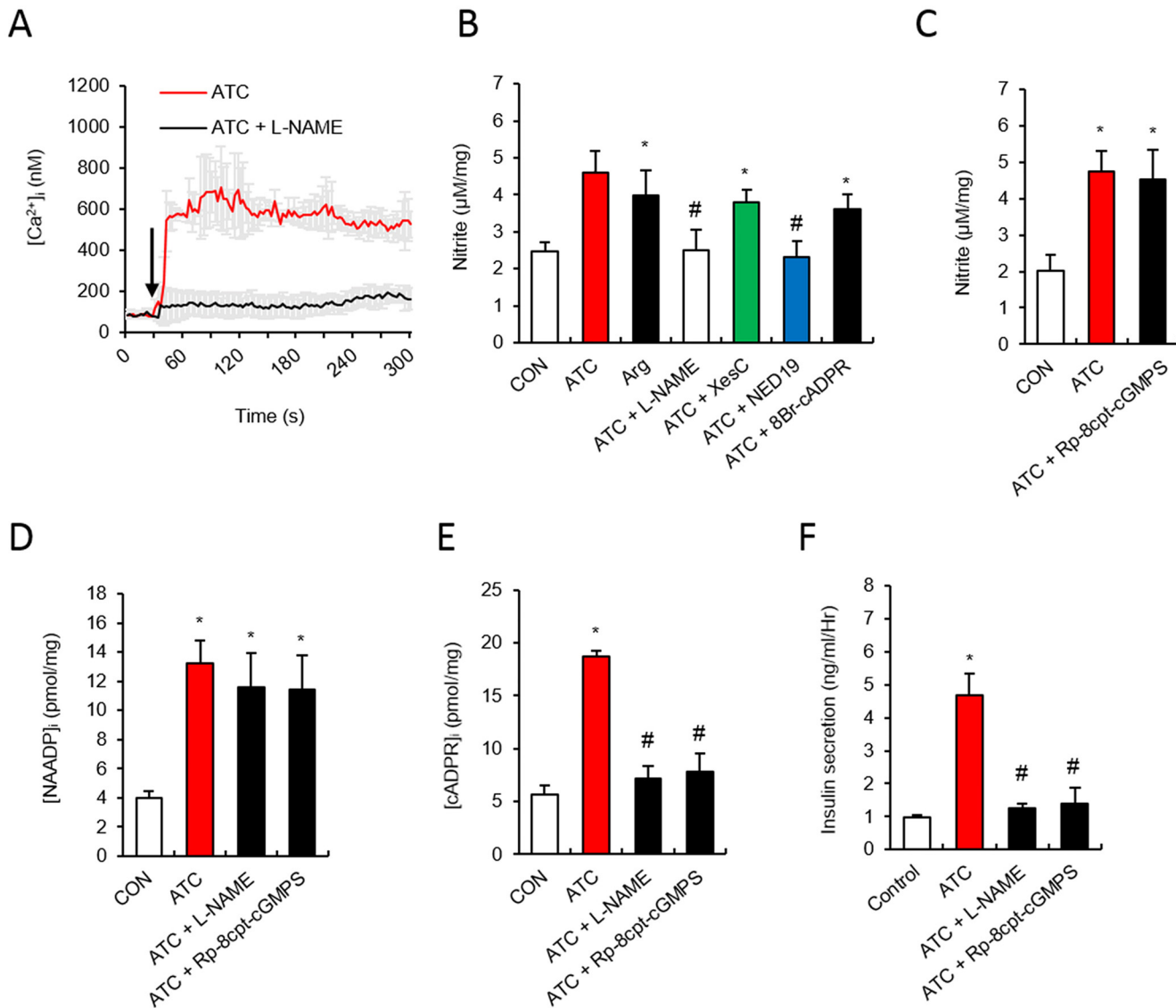


**Fig 4. NOS involves in ATC-induced cADPR formation but not in NAADP formation in pancreatic  $\beta$  cell.** (A) Effect of L-NG-Nitroarginine Methyl Ester (L-NAME) (5 mM) on ATC-induced  $Ca^{2+}$  signal. (B) Effect of L-NAME and  $Ca^{2+}$  second messenger inhibitors on ATC-induced nitrite formation. (C) Effect of cGMP antagonist, (Rp)-8-pCPT-cGMPs (20  $\mu$ M) on ATC-induced NO formation. (D and E) Effect of L-NAME and cGMP antagonist on ATC-induced cADPR and NAADP formation. (F) Effect of L-NAME and cGMP antagonists on ATC-induced insulin secretion. \*,  $P < 0.05$  versus CON level. #,  $P < 0.05$  versus ATC treated level. All data are expressed as the Mean  $\pm$  SEM.

doi:10.1371/journal.pone.0134962.g004

comparing  $Ca^{2+}$  signals in  $CD38^{+/+}$  and  $CD38^{-/-}$  mice upon treatment with ATC. Islet cells from  $CD38^{-/-}$  mice showed markedly reduced levels of sustained  $Ca^{2+}$  signals, compared to those from  $CD38^{+/+}$  mice (Fig 6A). To further confirm which second messenger was responsible for the difference in ATC-induced increases in  $Ca^{2+}$  levels in  $CD38^{+/+}$  and  $CD38^{-/-}$  mice, we measured NAADP and cADPR levels in both  $CD38^{+/+}$  and  $CD38^{-/-}$  islets after treatment with ATC. cADPR levels were decreased in  $CD38^{-/-}$  islets when compared to wild type islets upon ATC treatment, whereas NAADP levels in  $CD38^{-/-}$  islets were the same as those in wild type islets after ATC treatment (Fig 6B and 6C). ATC-induced formation of cAMP and NO, both signalling molecules upstream to CD38, displayed no difference between  $CD38^{+/+}$  and  $CD38^{-/-}$  islets (Fig 6D and 6E). ATC-induced insulin secretion was decreased in  $CD38^{-/-}$  islets

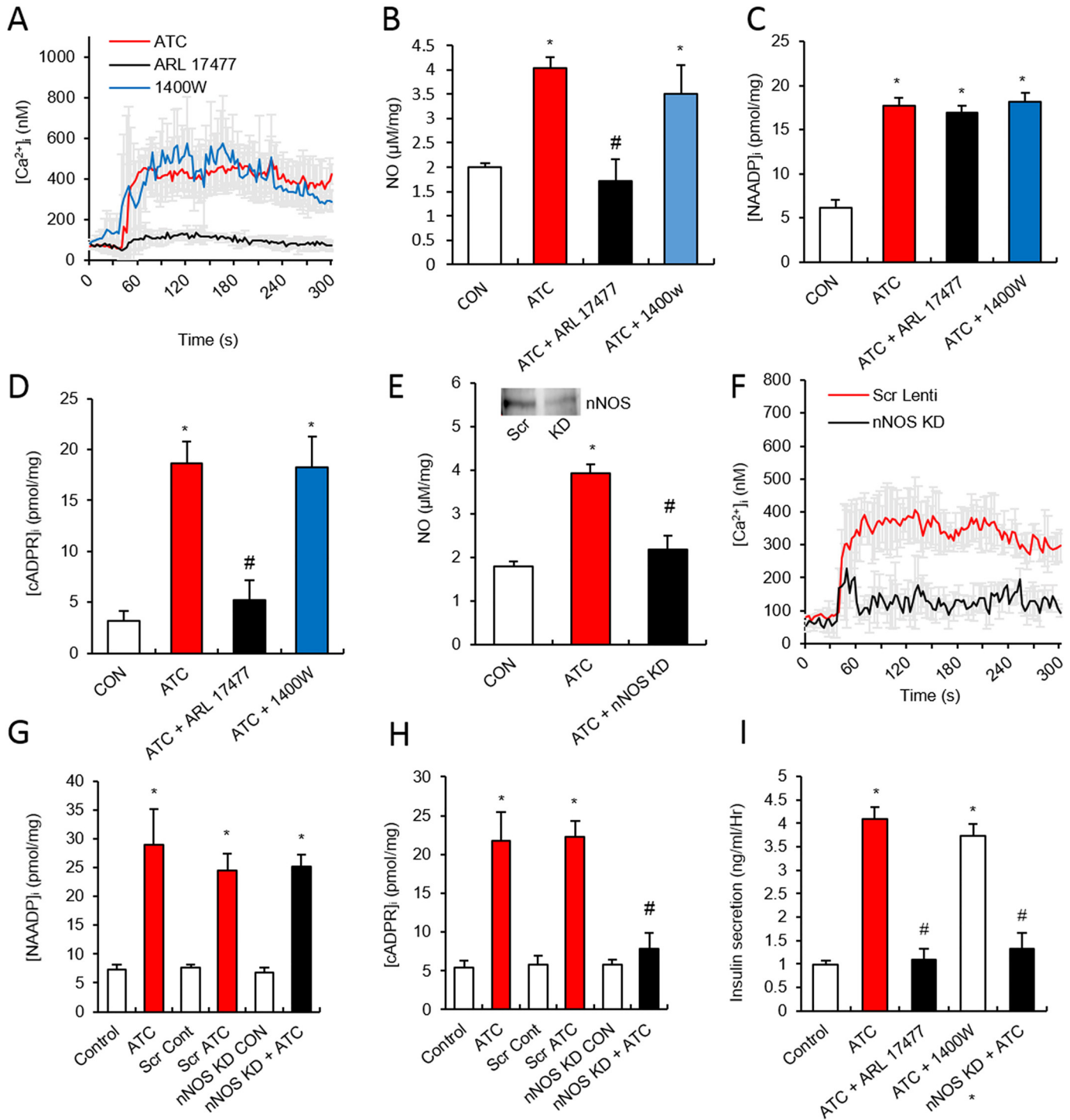


**Fig 5. nNOS plays a major role in ATC-induced  $Ca^{2+}$  signaling and insulin secretion in pancreatic  $\beta$  cell.** (A) Effect of nNOS inhibitor, ARL17477 (30  $\mu M$ ) and iNOS inhibitor, 1400W (100  $\mu M$ ) on ATC-induced  $Ca^{2+}$  signals. (B-D) Effect of nNOS and iNOS inhibitors on ATC-induced NO, cADPR, NAADP formation. (E) Effect of nNOS knock down (KD) on ATC-induced NO formation. (inset) Representative immunoblots for quantifications of nNOS protein expression in pancreatic  $\beta$  cell after infection with lentiviral particles expressing scrambled or nNOS-specific short hairpin (shRNA). (F) Effect of nNOS KD on ATC-induced  $Ca^{2+}$  signal. (G and H) Effects of nNOS KD on ATC-induced cADPR and NAADP formation. (I) Effect of nNOS inhibitors and nNOS KD on ATC-induced insulin secretion. \*,  $P < 0.05$  versus CON level. #,  $P < 0.05$  versus ATC treated level. All data are expressed as the Mean  $\pm$  SEM.

doi:10.1371/journal.pone.0134962.g005



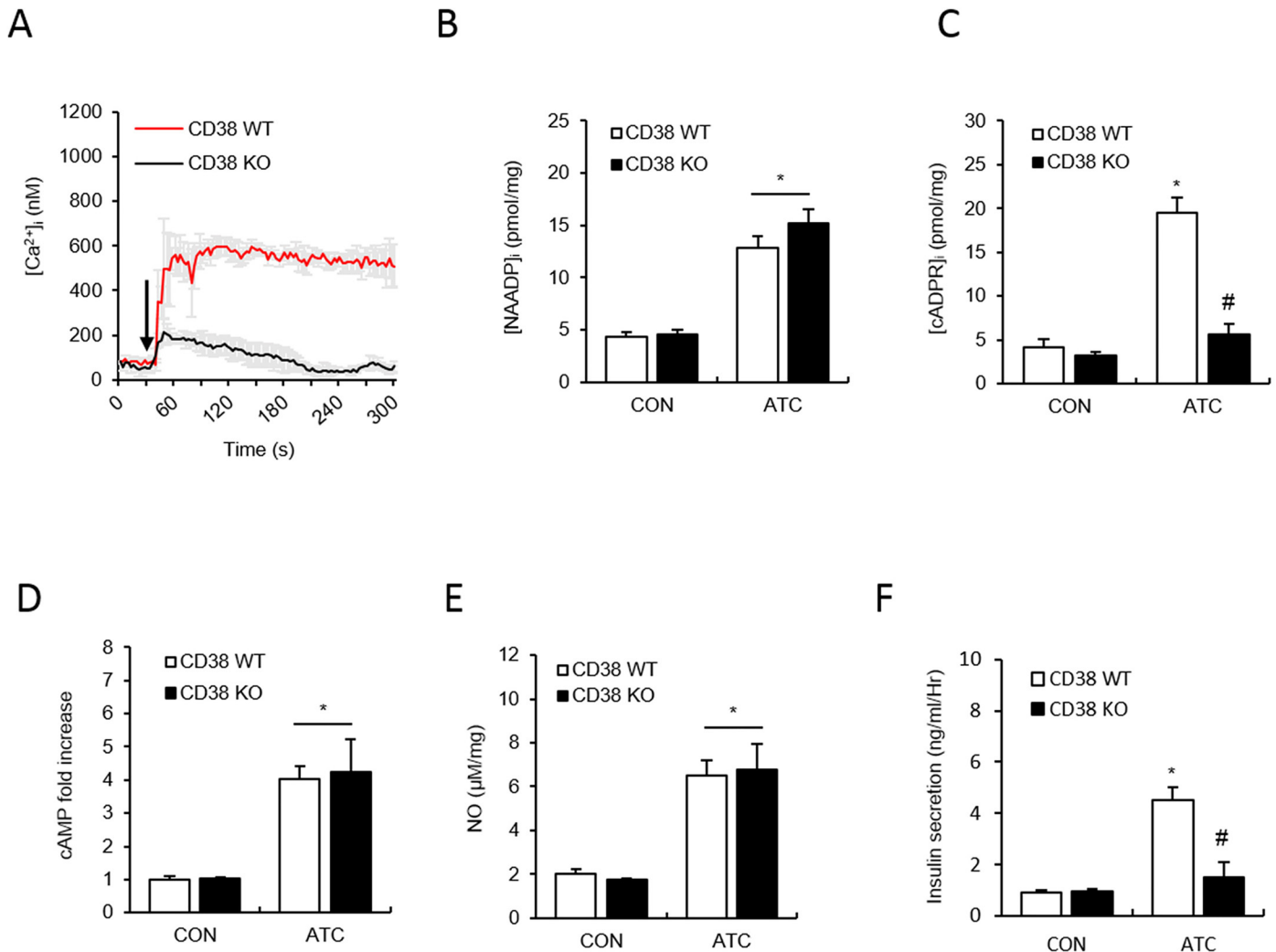


**Fig 6. ATC-induced Ca<sup>2+</sup> signals, cADPR and NAADP production, and insulin secretion in pancreatic β cell from wild-type (WT) and CD38 knock-out (KO) mice.** (A) Representative tracings of the Ca<sup>2+</sup> response to ATC in pancreatic β cell prepared from WT and CD38 KO mice. (B and C) ATC-stimulated NAADP and cADPR formation in WT and CD38 KO mice. (D and E) ATC-stimulated cAMP and NO formation in WT and CD38 KO mice. (F) ATC-stimulated insulin secretion in WT and CD38 KO mice. \*, P<0.05 versus CON level. #, P<0.05 versus ATC treated level. All data are expressed as the Mean ± SEM.

doi:10.1371/journal.pone.0134962.g006

(Fig 6F), indicating that CD38-mediated cADPR production plays an important role in ATC-induced insulin secretion.

## Discussion

In this study, we showed that a hybrid compound, ATC, induced an increase in Ca<sup>2+</sup> levels via the sequential production of two Ca<sup>2+</sup> second messengers: NAADP and cADPR. One component of ATC, TC, increased the production of cAMP, which induced NAADP synthesis. The resulting NAADP-mediated Ca<sup>2+</sup> rise induced the activation of NOS. NO activated GC to produce cGMP, which led to PKG activation. PKG induced CD38 activation to produce cADPR. The other component of ATC, L-arginine, served as a substrate for NOS, augmenting the signals of NAADP-mediated NOS activation (Fig 7). This hybrid compound showed a powerful

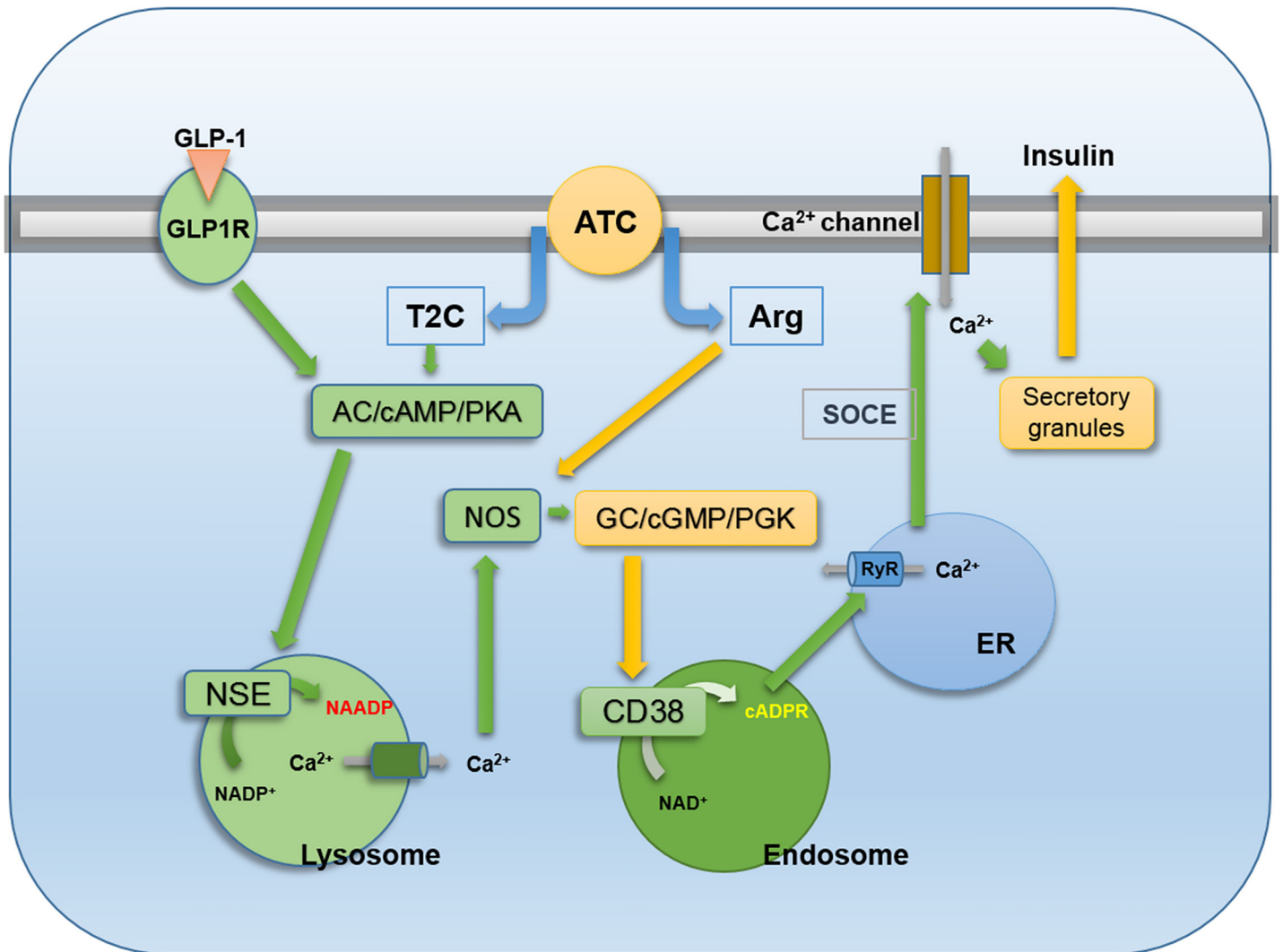


**Fig 7. Schematic representation of ATC-induced insulin secretion via cADPR and NAADP production as well as role of NO in pancreatic  $\beta$  cell.** Arginine Thiocarbonyl Carboxylate (ATC) enters and is divided into TC and arginine. TC contributes for Glutathione (GSH) formation, which stimulates adenylyl cyclase, resulting in the production of cAMP. cAMP/PKA activates NSE to produce NAADP, releasing  $\text{Ca}^{2+}$  from lysosome-related acidic organelles. NAADP-mediated increase of intracellular  $\text{Ca}^{2+}$  levels results in the activation of NOS. At this moment, arginine is provided as a substrate for Nitric Oxide synthase (NOS). Resulting Nitric Oxide (NO) synthesis activate guanylyl cyclase (GC)/protein kinase G (PKG). PKG activates CD38 to produce cADPR. cADPR-mediated  $\text{Ca}^{2+}$  release from the ER  $\text{Ca}^{2+}$  stores. cADPR-mediated  $\text{Ca}^{2+}$  release regulates the  $\text{Ca}^{2+}$  influx through store-operated  $\text{Ca}^{2+}$  entry (SOCE), resulting in insulin secretion in pancreatic  $\beta$  cells. GLP-1, an insulin secretion inducing hormone, also uses similar  $\text{Ca}^{2+}$  signalling pathway for insulin secretion in pancreatic  $\beta$  cells.

doi:10.1371/journal.pone.0134962.g007

insulin releasing effect in pancreatic islets when compared to other precursor molecules (Fig 1).

Cysteine is a rate-limiting precursor for the synthesis of GSH and intracellular GSH level is regulated by the availability of cysteine [39]. OTC and TC are the prodrugs of cysteine, and they can raise the plasma concentration of cysteine and the intracellular concentrations of cysteine and GSH [40–42]. We demonstrated OTC is an effective antidiabetic drug by inducing insulin secretion via CD38 internalization, cADPR formation, and subsequent  $\text{Ca}^{2+}$  rise [2].

This suggested that the cellular reducing system may involve the internalization of CD38 and the formation of cADPR, resulting in insulin secretion. GSH is known to be an activator of

adenylyl cyclase [36,43]. As predicted, ATC increased intracellular GSH levels as well as cAMP levels. ATC-induced NAADP and cADPR formation were dependent on cAMP (Fig 3A, 3F and 3G), indicating that cAMP may be upstream to NAADP formation, because cADPR formation is downstream to NAADP-induced  $Ca^{2+}$  signaling (Fig 2A and 2F). Therefore, our previous finding that OTC-induced CD38 internalization, resulting in cADPR formation [2], might be attributable to the downstream effect of NAADP formation through GSH-dependent cAMP generation.

Earlier studies showed that OTC is more potent than N-acetylcysteine in increasing reduced glutathione levels [44,45]. It was also found to block airway hyper-responsiveness and inflammation in an asthmatic animal model [46]. Here we found that ATC, a hybrid compound, is more effective in terms of insulin secretion, compared to OTC. ATC was used in the treatment of chronic hepatitis in 1980's [1]. However, its role in insulin secretion has not been studied. We found that ATC itself induced a rise in  $Ca^{2+}$ , attributable to the induction of the production of second messengers, NAADP and cADPR, in a sequential manner, which is analogous to that of GLP-1 [21]: When GLP-1 binds to GLP-1R, the stimulatory G protein activates adenylyl cyclase. The resulting production of cAMP induces NAADP synthesis, followed by cADPR formation. The sequential action of these  $Ca^{2+}$  second messengers results in  $Ca^{2+}$  signals that induce the release of insulin in pancreatic islets. Another analogous feature is the lack of involvement of  $IP_3$  in both signalling pathways (Fig 2B). Therefore, ATC is likely a physiological insulin secretory hormone mimic. Moreover, ATC supplies L-arginine, which is known to have insulin secretory potential [3,4]. This was confirmed by data showing that ATC is more potent in inducing  $Ca^{2+}$  signals, the production of  $Ca^{2+}$  second messengers, and insulin secretion, when compared to T2C and OTC (Fig 1).

Our data demonstrated that ATC as an arginine provider is a potent NOS activator (Fig 4B). The ATC-mediated NOS activation was found to be NOS isoform-specific in pancreatic islets; ATC activates nNOS preferentially, but not iNOS (Fig 5). Our data showed that NOS is upstream to cADPR formation and downstream to NAADP formation (Fig 5G and 5H), indicating that nNOS plays a role as a linker between the two  $Ca^{2+}$  second messengers. Based on our finding that cADPR is produced by CD38 (Fig 6C), NOS is important for the activation of CD38 in cADPR production. The NO-mediated activation of CD38 likely occurs via cGMP/PKG (Fig 4C–4E). Previously, we demonstrated that CD38 is internalized in a PKG-dependent manner through the phosphorylation of myosin heavy chain IIA, resulting in cADPR formation in lymphokine-activated killer (LAK) cells [47]. Since OTC induced CD38 internalization in pancreatic islets [2], ATC might also induce CD38 internalization.

Regarding the question of whether CO, another kind of gaseous transmitter, can induce insulin release, its role as a gaseous transmitter in the insulin secretion pathway has been proved in previous studies as follows: Hemin, the natural substrate for heme oxygenase (HO), increased  $[Ca^{2+}]_i$  transients in  $\beta$ -cells, and Zn-protoporphyrin, a HO inhibitor, inhibited glucose-stimulated insulin release from pancreatic islets [48]. As both CO and NO act on guanylate cyclase to generate cGMP [49], it is interesting to see the causal relationship of the two gaseous transmitters. Crosstalk between the signaling pathways of the two transmitters has been studied: NO and NO-related species induce HO-1 expression [49], suggesting that CO is involved in insulin secretion as an active messenger, and that NO may act via the activation or induction of HO. Regarding the action of H<sub>2</sub>S, the third gaseous transmitter, on the secretion of insulin from pancreatic  $\beta$ -cells, it has been reported that this gaseous transmitter inhibits insulin release [50,51]. On the other hand, H<sub>2</sub>S reduces the cellular stress evoked by glucose, possibly through its anti-oxidant properties [52].

Concerning the question of whether ATC additively stimulates insulin release in the presence of simultaneous sulfonylurea (SU) or GLP-1 treatment, our data showed that the

combined treatment of ATC with SU or GLP-1 had a higher efficacy than any singular treatment (S5 Fig), suggesting that ATC may use different pathways from those utilized by SU or GLP-1 for insulin secretion. Regarding insulin secretion stimulation potency, ATC and SU were comparable (S5 Fig).

Given that NAADP has demonstrated auto/paracrine functions in vivo and in vitro [53,54], it can be assumed that NAADP released from pancreatic islets upon stimulation with ATC plays a beneficial role by acting on the peripheral tissues, such as adipose tissues. Since NAADP is a  $\text{Ca}^{2+}$  messenger that is essential for glucose uptake in adipose tissues [55], it is expected that ATC-induced NAADP formation in pancreatic islets results in an ameliorating effect in glucose homeostasis via paracrine functions.

One of the notable findings in this study is the existence of a novel NAADP-synthesizing enzyme other than CD38 as evidenced by data showing that islets from CD38<sup>-/-</sup> mice showed no impairment in NAADP formation upon ATC treatment, compared to those from wild type mice (Fig 6B). Because CD38 is capable of producing NAADP as well as cADPR [29,56], it is quite interesting to see why two different enzymes participate in ATC-induced insulin secretion in pancreatic islets.  $\beta$ -adrenergic agonist-stimulated cardiomyocytes have also displayed similar NAADP-synthesizing enzymes and CD38 for NAADP and cADPR production, respectively (Gul *et al.* unpublished).

In conclusion, we have demonstrated that ATC, an arginine-containing prodrug of cysteine, induces insulin secretion via  $\text{Ca}^{2+}$  signalling messenger formation in mice. ATC is a likely physiological agent, because it harnesses the cellular signalling system to increase intracellular  $\text{Ca}^{2+}$  levels, resulting in insulin secretion. Our results imply that ATC has the potential to be applied as an ideal anti-diabetic drug.

## Supporting Information

**S1 Fig. The chemical structural formulas of ATC, T2C, Arg and OTC.** 1: Oxothiazolidine-4-carboxylic acid (OTC), 2: Thiazolidine-2-carboxylic acid (T2C), 3: Thiazolidine-4-carboxylic acid (T4C), 4: Arginine, 5: Arginine thiazolidine-2-carboxylic acid (ATC), 6: Arginine thiazolidine-4-carboxylic acid (ATC).

(PDF)

**S2 Fig. Prodrug, Thiazolidine-2-carboxylic acid (T2C) has more effective to produce GSH than Thiazolidine-4-carboxylic acid (T4C) in pancreatic  $\beta$  cell.** \*,  $P < 0.05$  versus CON GSH level. #,  $P < 0.05$  versus T2C treated GSH level. All data are expressed as the Mean  $\pm$  SEM.

(PDF)

**S3 Fig. ATC-induced cADPR and NAADP production in pancreatic  $\beta$  cell.** Islets were treated with/without ATC (100, 400, 700  $\mu\text{M}$ , and 1  $\mu\text{M}$ ) and measured cADPR (A) and NAADP (B) levels. \*,  $P < 0.05$  versus CON cADPR and NAADP level. All data are expressed as the Mean  $\pm$  SEM.

(PDF)

**S4 Fig. Effect of RYR inhibitor (20  $\mu\text{M}$  Ryanodine) on ATC-induced  $\text{Ca}^{2+}$  signals.**

(PDF)

**S5 Fig. Effect of ATC, SU, GLP-1 and combined treatment on insulin secretion in pancreatic islets.** \*,  $P < 0.05$  versus CON insulin secretion level. #,  $P < 0.05$  versus ATC complex treated level. All data are expressed as the Mean  $\pm$  SEM.

(PDF)

## Acknowledgments

We thank Chansu Park for critically reading the manuscript.

## Author Contributions

Conceived and designed the experiments: UHK. Performed the experiments: AIS DRP TGH KHP SYK. Analyzed the data: UHK. Contributed reagents/materials/analysis tools: SYK. Wrote the paper: AIS DRP UHK.

## References

1. Bramato C, Salassa B, Soranzo ML, Bosio G, Andreoni G. Use of arginine thiazolidine carboxylate in the treatment of chronic hepatitis. Preliminary findings. *Minerva Dietol Gastroenterol* 1982 28: 65–70. PMID: [7043311](#)
2. Han MK, Kim SJ, Park YR, Shin YM, Park HJ, Park KJ, et al. Antidiabetic effect of a prodrug of cysteine, L-2-oxothiazolidine-4-carboxylic acid, through CD38 dimerization and internalization. *J Biol Chem* 2002 277: 5315–5321. PMID: [11679582](#)
3. Schmidt HH, Warner TD, Ishii K, Sheng H, Murad F. Insulin secretion from pancreatic  $\beta$ -cells caused by L-arginine-derived nitrogen oxides. *Science* 1992 255:721–723. PMID: [1371193](#)
4. Thams P, Capito K. L-Arginine stimulation of glucose-induced insulin secretion through membrane depolarization and independent of nitric oxide. *Eur J Endocrinol* 1999 140: 87–93. PMID: [10037257](#)
5. Furchgott RF, Zawadzki JV. The obligatory role of endothelial cells in the relaxation of arterial smooth muscle by acetylcholine. *Nature* 1980 288: 373–376. PMID: [6253831](#)
6. Willmott NJ, Galione A, Smith PA. Nitric oxide induces intracellular  $Ca^{2+}$  mobilization and increases secretion of incorporated 5-hydroxytryptamine in rat pancreatic beta-cells. *FEBS Lett* 1995 371: 99–104. PMID: [7672132](#)
7. Kong SK, Choy YM, Lee CY. The nitric oxide donor, sodium nitroprusside, increased intranuclear and cytosolic free calcium concentration in single PU5-1.8 cells. *Biochem Biophys Res Commun* 1994 199: 234–240. PMID: [8123018](#)
8. Willmott N, Sethi JK, Walseth TF, Lee HC, White AM, Galione A. Nitric oxide-induced mobilization of intracellular calcium via the cyclic ADP-ribose signaling pathway. *J Biol Chem* 1996 271: 3699–3705. PMID: [8631983](#)
9. Ward WK, Bolgiano DC, McKnight B, Halter JB, Porte D Jr. Diminished B Cell Secretory Capacity in Patients with Non-insulin dependent Diabetes Mellitus. *J Clin Invest* 1984 74: 1318–1328. PMID: [6384269](#)
10. Lee HC. Cyclic ADP-ribose and NAADP: fraternal twin messengers for calcium signaling. *Sci China Life Sci* 2011 54: 699–711. doi: [10.1007/s11427-011-4197-3](#) PMID: [21786193](#)
11. Malavasi F, Deaglio S, Funaro A, Ferrero E, Horenstein AL, Ortolan E, et al. Evolution and function of the ADP ribosyl cyclase/CD38 gene family in physiology and pathology. *Physiol Rev* 2008 88: 841–886. doi: [10.1152/physrev.00035.2007](#) PMID: [18626062](#)
12. Lee HC, Aarhus R. ADP-ribosyl cyclase: an enzyme that cyclizes NAD<sup>+</sup> into a calcium-mobilizing metabolite. *Cell Regul* 1991 2: 203–209. PMID: [1830494](#)
13. Glick DL, Hellmich MR, Beushausen S, Tempst P, Bayley H, Strumwasser F. Primary structure of a molluscan egg-specific NADase, a second-messenger enzyme. *Cell Regul* 1991 2: 211–218. PMID: [1650255](#)
14. States DJ, Walseth TF, Lee HC. Similarities in amino acid sequences of Aplysia ADP-ribosyl cyclase and human lymphocyte antigen CD38. *Trends Biochem Sci* 1992 17: 495.
15. Lee HC. Structure and Enzymatic Functions of Human CD38. *Mol Med* 2006 12:317–323. PMID: [17380198](#)
16. Takasawa S, Nata K, Yonekura H, Okamoto H. Cyclic ADP-ribose in insulin secretion from pancreatic beta cells. *Science* 1993 259: 370–373. PMID: [8420005](#)
17. An NH, Han MK, Um C, Park BH, Park BJ, Kim HK et al. Significance of ecto-cyclase activity of CD38 in insulin secretion from mouse pancreatic islet cells. *Biochem Biophys Res Commun* 2001 282: 781–786. PMID: [11401531](#)
18. Masgrau R, Churchill GC, Morgan AJ, Ashcroft SJ, Galione A. NAADP: a new second messenger for glucose-induced  $Ca^{2+}$  responses in clonal pancreatic beta cells. *Curr Biol* 2003 13: 247–251. PMID: [12573222](#)



19. Johnson JD, Misler S. Nicotinic acid-adenine dinucleotide phosphate-sensitive calcium stores initiate insulin signaling in human beta cells. *Proc Natl Acad Sci USA* 2002 99: 14566–14571. PMID: [12381785](#)
20. Mitchell KJ, Lai FA, Rutter GA. Ryanodine receptor type I and nicotinic acid adenine dinucleotide phosphate receptors mediate Ca<sup>2+</sup> release from insulin containing vesicles in living pancreatic beta-cells (MIN6). *J Biol Chem* 2003 278: 11057–11064. PMID: [12538591](#)
21. Kim BJ, Park KH, Yim CY, Takasawa S, Okamoto H, Im MJ, et al. Generation of nicotinic acid adenine dinucleotide phosphate and cyclic ADP-ribose by glucagon-like peptide-1 evokes Ca<sup>2+</sup> signal that is essential for insulin secretion in mouse pancreatic islets. *Diabetes* 2008 57: 868–878. doi: [10.2337/db07-0443](#) PMID: [18184929](#)
22. Kim HL, Yoon HJ, Ha JY, Lee BI, Lee HH, Mikami B, et al. Crystallization and preliminary X-ray crystallographic analysis of nicotinic acid mononucleotide adenylyltransferase from *Pseudomonas aeruginosa*. *Acta Crystallogr D Biol Crystallogr* 2004 60: 948–949. PMID: [15103148](#)
23. Institute of Laboratory Animal Research, Commission of Life Sciences, National Research Council. *Guide of the care and use of laboratory animals*. Washington DC: National Academy Press 1996.
24. Rah SY, Park KH, Han MK, Im MJ, Kim UH. Activation of CD38 by interleukin-8 signaling regulates intracellular Ca<sup>2+</sup> level and motility of lymphokine-activated killer cells. *J Biol Chem* 2009 280: 2888–2895.
25. Tsien RY, Pozzan T, Rink TJ. T-cell mitogens cause early changes in cytoplasmic free Ca<sup>2+</sup> and membrane potential in lymphocytes. *Nature* 1982 295: 68–71. PMID: [6799829](#)
26. Schuit FC, Pipeleers DG. Regulation of adenosine 3',5'-monophosphate levels in the pancreatic B cell. *Endocrinology* 1985 117: 834–840. PMID: [2410241](#)
27. Graeff RM, Lee HC. High throughput fluorescence based assays for cyclic ADP-ribose, NAADP, and their metabolic enzymes. *Comb Chem High Throughput Screen* 2003 6: 367–379. PMID: [12769681](#)
28. Cho YS, Han MK, Kwark OS, Phoe MS, Cha YS, An NH, et al. Auto-ADP-ribosylation of NAD glycohydrolase from *Neurospora crassa*. *Comp Biochem Physiol B Biochem Mol Biol* 1998 120: 175–181. PMID: [9787786](#)
29. Lee HC, Aarhus R. ADP-ribosyl cyclase: an enzyme that cyclizes NAD<sup>+</sup> into a calcium-mobilizing metabolite. *Cell Regul* 1991 2: 203–209. PMID: [1830494](#)
30. You H, Laychock SG. Long-term treatment with atrial natriuretic peptide inhibits ATP production and insulin secretion in rat pancreatic islets. *Am J Physiol Endocrinol Metab* 2011 300: E435–E444. doi: [10.1152/ajpendo.00398.2010](#) PMID: [20959527](#)
31. Hibbs JB Jr, Taintor RR, Vavrin Z, Rachlin EM. Nitric oxide: a cytotoxic activated macrophage effector molecule. *Biochem Biophys Res Commun* 1988 157: 87–94. PMID: [3196352](#)
32. Marletta MA, Yoon PS, Iyengar R, Leaf CD, Wishnok JS. Macrophage oxidation of L-arginine to nitrite and nitrate: nitric oxide is an intermediate. *Biochemistry* 1988 27: 8706–8711. PMID: [3242600](#)
33. Han MK, Yim CY, An NH, Kim HR, Kim UH. Glycosylphosphatidylinositol-anchored NAD glycohydrolase is released from peritoneal macrophages activated by interferon-gamma and lipopolysaccharide. *J Leukoc Biol* 1994 56: 792–796. PMID: [7996054](#)
34. Fitzpatrick PF, Massey V. Thizaolidine-2-carboxylic acid, an adduct of cysteamine and glyoxylate, as a substrate for D-amino acid oxidase. *J Biol Chem* 1982 257: 1166–1171. PMID: [6120164](#)
35. Wlodek L, Rommelspacher H, Susilo R, Radomski J, Höfle G. Thiazolidine derivatives as source of free L-cysteine in rat tissue. *Biochem Pharmacol* 1993 46: 1917–1928. PMID: [8267641](#)
36. Ammon HP, Heinzl S, Abdel-Hamid M, Kallenberger HM, Hagenloh I. Effect of Diamide and Reduced Glutathione on the Elevated Levels of Cyclic AMP in Rat Pancreatic Islets Exposed to Glucose, p-Chloromercuribenzoate and Aminophylline. *Naunyn-Schmiedeberg's Arch Pharmacol* 1982 319: 243–248.
37. Friebe A, Koesling D. Regulation of nitric oxide-sensitive guanylyl cyclase. *Circ Res* 2003 93:96e105.
38. Looms DK, Tritsarlis K, Nauntofte B, Dissing S. Nitric oxide and cGMP activate Ca<sup>2+</sup>-release processes in rat parotid acinar cells. *Biochem J* 2001 355: 87–95. PMID: [11256952](#)
39. Lu SC. Regulation of hepatic glutathione synthesis: current concepts and controversies. *FASEB J* 1999 13: 1169–1183. PMID: [10385608](#)
40. Vita JA, Frei B, Holbrook M, Gokce N, Leaf C, Keaney JF Jr. L-2-Oxothiazolidine-4-carboxylic acid reverses endothelial dysfunction in patients with coronary artery disease. *J Clin Invest* 1988 101: 1408–1414.
41. Oiry J, Puy JY, Mialocq P, Clayette P, Fretier P, Jaccard P, et al. Synthesis and in vitro anti-HIV activity in human monocyte-derived macrophages of 2-oxothiazolidine-4(R)-carboxylic acid derivatives. *J Med Chem* 1999 42: 4733–4740. PMID: [10579837](#)

42. Porta P, Aebi S, Summer K, Lauterburg BH. L-2-oxothiazolidine-4-carboxylic acid, a cysteine prodrug: pharmacokinetics and effects on thiols in plasma and lymphocytes in human. *J Pharmacol Exp Ther* 1991 257: 331–334. PMID: [2019996](#)
43. Mukherjee SP, Lynn WS. Role of cellular redox state and glutathione in adenylate cyclase activity in rat adipocytes. *Biochim Biophys Acta* 1979 568: 224–233. PMID: [444543](#)
44. Williamson JM, Meister A. Stimulation of hepatic glutathione formation by administration of L-2-oxothiazolidine-4-carboxylate, a 5-oxo-l-prolinase substrate. *Proc Natl Acad Sci USA*. 1981 78: 936–939. PMID: [6940159](#)
45. Mesina JE, Page RH, Hetzel FW, Chopp M. Administration of l-2-oxothiazolidine-4-carboxylate increases glutathione levels in rat brain. *Brain Res* 1989 478: 181–183. PMID: [2924114](#)
46. Lee YC, Lee KS, Park SJ, Park HS, Lim JS, Park KH, et al. Blockade of airway hyperresponsiveness and inflammation in a murine model of asthma by a prodrug of cysteine, l-2-oxothiazolidine-4-carboxylic acid. *FASEB J* 2004 18: 1917–1919. PMID: [15385436](#)
47. Rah SY, Park KH, Nam TS, Kim SJ, Kim H, Im MJ, et al. Association of CD38 with nonmuscle myosin heavy chain IIA and Lck is essential for the internalization and activation of CD38. *J Biol Chem* 2007 282: 5653–5660. PMID: [17182620](#)
48. Lundquist I, Alm P, Salehi A, Henningsson R, Grapengiesser E, Hellman B. Carbon monoxide stimulates insulin release and propagates  $Ca^{2+}$  signals between pancreatic  $\beta$ -cells. *Am J Physiol* 2003 285: E1055–E1063.
49. Kim YM, Pae HO, Park JE, Lee YC, Woo JM, Kim NH, et al. Heme Oxygenase in the Regulation of Vascular Biology: From Molecular Mechanisms to Therapeutic Opportunities. *Antioxid Redox Signal* 2011 14:137–167 doi: [10.1089/ars.2010.3153](#) PMID: [20624029](#)
50. Kaneko Y, Kimura Y, Kimura H, Niki I. L-Cysteine Inhibits Insulin Release From the Pancreatic  $\beta$ -cell. *Diabetes* 2006 55:1391–1397. PMID: [16644696](#)
51. Tang G, Zhang L, Yang G, Wu L, Wang R. Hydrogen sulfide-induced inhibition of L-type  $Ca^{2+}$  channels and insulin secretion in mouse pancreatic beta cells. *Diabetologia* 2013 56:533–541. doi: [10.1007/s00125-012-2806-8](#) PMID: [23275972](#)
52. Kaneko Y, Kimura T, Taniguchi S, Souma M, Kojima Y, Kimura H, et al. Glucose-induced production of hydrogen sulfide may protect the pancreatic beta-cells from apoptotic cell death by high glucose. *FEBS Lett* 2009 583:377–382. doi: [10.1016/j.febslet.2008.12.026](#) PMID: [19100738](#)
53. Billington RA, Bellomo EA, Floriddia EM, Erriquez J, Distasi C, Genazzani AA. A transport mechanism for NAADP in a rat basophilic cell line. *FASEB J* 2006 20: 521–523. PMID: [16403787](#)
54. Park KH, Kim BJ, Shahl AI, Han MK, Lee HC, Kim UH. Autocrine/paracrine function of NAADP for glucose homeostasis in pancreatic  $\beta$  cells and adipocytes. *J Biol Chem* 2013 288: 35548–35558. doi: [10.1074/jbc.M113.489278](#) PMID: [24165120](#)
55. Song EK, Lee YR, Kim YR, Yeom JH, Yoo CH, Kim HK, et al. NAADP mediates insulin-stimulated glucose uptake and insulin sensitization by PPAR $\gamma$  in adipocytes. *Cell Rep* 2012 2: 1607–1619. doi: [10.1016/j.celrep.2012.10.018](#) PMID: [23177620](#)
56. Aarhus R, Graeff RM, Dickey DM, Walseth TF, Lee HC. ADP-ribosyl cyclase and CD38 catalyze the synthesis of a calcium mobilizing metabolite from NADP. *J Biol Chem* 1995 270: 30327–30333. PMID: [8530456](#)